Accepted paper: https://doi.org/10.1016/j.mseb.2019.04.013
Materials Science and Engineering: B
Advanced Functional Solid-state Materials 243 (2019) 175-182

The initial characteristics of the polypyrrole based aqueous rechargeable batteries with supercapattery characteristics

Branimir N. Grgur[1,*], Marija Janačković[1,2], Branimir Z. Jugović[3], Milica M. Gvozdenović[1],

[1]Faculty of Technology and Metallurgy,
University of Belgrade, Karnegijeva 4, Belgrade, Serbia
[2]Faculty of Technical Sciences, Kneza Miloša 7, Kosovska Mitrovica, Serbia
[3]Institute of Technical Sciences of the Serbian Academy of Sciences and Arts, Knez Mihailova 35/IV, Belgrade, Serbia

*Corresponding author:
E-mail address: BNGrgur@tmf.bg.ac.rs
Phone/fax: +381 11 3303681

Abstract

The electrochemically synthesized polypyrrole (PPy) is investigated as a possible active material of the low-cost aqueous based secondary power sources in combination with zinc, lead oxide, and lead sulfate. The discharge capacity of the polypyrrole in the chloride-based electrolyte (for the Zn|PPy cell) is in the range 110 mAh g^{-1} of PPy, while in the sulfate-based electrolyte ~150 mAh g^{-1} of PPy (for the $PbSO_4$|PPy and PPy|PbO_2 cells), which is close to the theoretically calculated values. Electrochemical and electrical parameters, reactions in the cells, specific capacity, specific capacitance, energy, and power, for the Zn|PPy, PPy|PbO_2 and

$PbSO_4$|PPy cells are determined. In addition, the energy efficiency, for the considered systems is estimated. Obtained values of the specific power and energy, could classified investigated systems as a battery type hybrid superacapacitors or "supercapattery".

Keywords: Zinc; Lead sulfate; Lead oxide; Power; Supercapattery

1. Introduction

Interest in the use of intrinsically conducting polymers (ICP's) for the preparation of electrodes in rechargeable power sources with aqueous electrolytes has a long history [1,2]. Although many different ICP were considered, polypyrrole proved to be particularly interesting due to its high specific doping/dedoping capacity of ~140 Ah g^{-1}, or ~90 Ah cm^{-3} [2], environmental acceptability, electrochemical reversibility and activity in a wide range of pH, ease of chemical and electrochemical synthesis etc. [3]. Most of the studies were dedicated to the application of PPy as an electrode material in supercapacitors [4, 5], cathodes in biocompatible power sources [6-8], in all-polymers based power sources [9] or as anode in the lithium intercalation battery based on aqueous electrolytes [3, 10-15]. The operational principle of a lithium battery is based on lithium ion intercalation/deintercalation from the positive electrode ($LiCoO_2$, $Li_2Mn_2O_4$) and doping/dedoping of the anions from ICP's negative electrode. During the discharge of a battery, lithium ions intercalate into the positive electrode, while the negative electrode is doped by the anions, and during the charge of the battery, the opposite reactions take places. Wang et al. investigated PPy|Mn_2O_4 and PPy|$LiCoO_2$ with saturated Li_2SO_4 electrolyte [11, 12]. They reported the open circuit voltage of 1.6 V and specific capacity of ~ 45 mAh g^{-1} for PPy|Mn_2O_4, while open circuit voltage of 1.2 V, the average discharge voltage of 0.8 V, and specific capacity of ~30 mAh g^{-1} were obtained for PPy|$LiCoO_2$ cell. Beside its favorable characteristics, lithium-based systems are limited by the high price of the lithium salts.

On the other hand, classical battery systems with aqueous electrolyte and zinc or lead electrodes in combination with PPy were not considered extensively [2, 6, 16-19]. We had previously reported simulated cell characteristics based on investigations of the half-cell reactions of Zn|PPy system in 0.1 M ammonium chloride containing 0.1 M sodium citrate and 0.07 M $ZnCl_2$ [17]. The voltage range during the charge of the cell was reported to be between 0.8 and 1.85 V, while discharge voltage in the range of 1.6 and 0.6 V. The specific discharge capacity of ~80 mAh g^{-1} was calculated taking into account active mass of PPy. A slight increase in PPy electrode capacity during charge/discharge cycles was also observed.

Polypyrrole is the well-known pseudocapacitive materials [4] that in the combinations with classical battery electrode could improve specific power of the cell retaining good specific energy [20].

Consequently, the aim of this investigation was to evaluated the initial electrochemical and electrical characteristics of PPy electrode coupled with zinc or lead/lead sulfate anodes and lead sulfate/lead oxide cathode in the classical battery system based on aqueous electrolytes. The main goal will be to determine the specific capacitance, energy and power of such relatively simple electrochemical systems.

2. Experimental

Polypyrrole (PPy) electrode was formed by electrochemical polymerization of pyrrole, at constant current density of 2 mA cm^{-2} (galvanostatically), from aqueous electrolyte containing 0.1 M pyrrole (p.a. Aldrich) and 1.0 M HCl or 1.0 M H_2SO_4 (p.a Merck) onto plane graphite electrode (1.5 cm × 4 cm, A = 6 cm^2). Polymerization charge was 12 mAh and 3.6 mAh for PPy obtained from chloride and sulfate acidic electrolytes, respectively. The experimentally determined masses of PPy by the measuring the weight of the electrode before and after electropolymerization were 14.4 mg and 5.2 mg. Prior to polymerization, pyrrole was distilled in an argon atmosphere. High purity zinc and lead (>99.9%, Alfa Aesar GmbH & Co KG, Germany) plates (1.5 cm ×4 cm, A = 6 cm^2) served as anode or cathode. Mechanical polishing of electrodes with fine emery papers (2/0, 3/0 and 4/0, respectively) followed by degreasing with acetone in an ultrasonic bath was always applied before experiments.

Modified Planté procedure was used for the formation of lead dioxide electrode. As previously reported, the process was carried out in 1.0 M H_2SO_4 (p.a Merck) and 0.05 M $KClO_4$ (p.a. Merck) [21]. Naturally, formed lead dioxide was removed from the lead electrode upon immersion in 8 M HNO_3 for 30 s, followed by rinsing with distilled water. Cathode pretreatment of the lead electrode at a constant current of 6 mA during 10 min was applied before galvanostatic oxidation with 6 mA in the same electrolyte. The remains of the perchlorate ions were removed by rinsing with bidistilled water. Finally, five successive oxidation and reduction processes with 12 mA during 500 s in pure 1 M H_2SO_4 were used for the formation of the electrode. The same process was used for the formation of lead sulfate electrode with the difference that the formed PbO_2 was reduced galvanostatically in 1 M H_2SO_4 to obtain Pb and then oxidized to $PbSO_4$. Using the Faraday law the mass of $PbSO_4$ is estimated to 5.4 mg, which corresponded to 4.3 mg of PbO_2. The investigation of the electrochemical characteristics of the zinc-polypyrrole cell was carried out in the aqueous electrolyte with 2.0 M NH_4Cl and 1.1 M

$ZnCl_2$ (p.a. Merck) while the polypyrrole-lead cell was tested in 1.0 M H_2SO_4 and 0.5 M $(NH_4)_2SO_4$ (p.a. Merck). Saturated calomel electrode was used as a reference, while corresponding metals as a counter electrode. Experiments were carried out with Gamry PC3 potentiostat/galvanostat, and digital voltmeter ISO-Tech IDM 73, RS-232 interfaced to a PC was used for recording of the cell voltage.

For the XRD study of as-synthesized PbO_2 and $PbSO_4$, the same procedure as for the electrode preparation was applied, only the oxidation was conducted for the 2000 s, to minimize the influence of pure lead from the electrode bulk. The XRD pattern of the samples was recorded with an Ital Structure APD2000 X-ray diffractometer in a Bragg–Brentano geometry using CuKα radiation and the step-scan mode (range: 10–90° 2θ, step-time: 0.50 s, step-width: 0.02°). Optical micrographs of the as synthetized materials were obtained with an optical microscope Olympus CX41 connected to PC.

3. Results and discussion

3.1. Electrochemical polymerization of pyrrole

Electrochemical polymerization of pyrrole on anode proceed simultaneously with the doping of the anions to achieve electroneutrality, according to [19, 22]:

$$n\mathrm{Py} + ny\mathrm{A}^{z-} = [\mathrm{PPy}^{zy+}(\mathrm{A}^{z-})_y]_n + 2n\mathrm{H}^+ + (2 + zy)n\mathrm{e} \quad (1)$$

where y refers to the degree of doping and z for a charge of the doping anions A^{z-}. Probably the most accepted mechanism of electrochemical polymerization of pyrrole was proposed by Diaz et al. [23]. At the beginning of the reaction, monomers are oxidized to primary cation radicals with delocalized charge. In further, rate-determining step, cation radicals form dimmers followed by ejection of two protons. The dimers are easier to oxidize due to greater conjugation length. The propagation of the polymer proceeds through the addition of newly formed cation radicals to oligomeric species.

Available charge of the PPy electrode can be obtained considering the charge of the polymerization process, Q_{pol}, which is given by [18]:

$$Q_{pol} = I_{pol}\, t_{pol} = (2 + zy)neF \quad (2)$$

The stoichiometry of the electrochemically synthesized PPy is $(2 + zy)$ meaning that charge of ~2.1F to 2.6F is consumed per mole of monomer [24]. 2F refers to the polymerization

processes (protons expelling), while extra charge of 0.1*F*-0.6*F* stands for the doping of the polymer chain. Theoretical available capacity for the p-doping/dedoping i.e. charge/discharge according to:

$$[\mathrm{PPy}]_n + nyA^{z-} = [\mathrm{PPy}^{zy+}(A^{z-})_y]_n + znye \quad (3)$$

is given by:

$$Q_{c,d} = It = nzyeF \quad (4)$$

The available capacity for the anion exchange can be connected to the polymerization charge by combining Eqs. (2) and (4):

$$Q_{c,d} = \frac{zy}{2+zy} Q_{pol} = \frac{zy}{2+zy} I_{pol} t_{pol} \quad (5)$$

In order to calculate the specific capacity of the PPy electrode, the active mass of the PPy has to be estimated. The mass of the PPy formed in the polymerization process is related to the polymerization charge according to:

$$m(\mathrm{PPy}) = \frac{I_{pol} t_{pol} [M_M - 2M_{H^+} + yM_A] p}{(2/\eta + zy)(p-1)F} \quad (6)$$

where η refers the polymerization current efficiency, p is the degree of polymerization, M_M and M_A are the molar masses of the pyrrole monomer unit, 67.09 g mol^{-1}, and the doping anion respectively, F is the Faraday constant. In a charge terms current efficiency is close to 100%; providing a possibility of controlling the mass and thickness of the polypyrrole film [24, 25].Taking into account that polymerization efficiency is η ~ 1, and a large value for p, theoretical specific capacity (Ah g^{-1}) of PPy can be obtained by combining Eqs (5) and (6):

$$q_{s,t} = \frac{zyF}{[M_M - 2M_{H^+} + yM_A]} \quad (7)$$

3.2. Zinc-polypyrrole system

Electrochemical formation of PPy electrode in hydrochloric acid based electrolyte and its characterization was given in Figure 1. Electrochemical polymerization of pyrrole occurred at the potential of ~ 0.7 V (inset in Fig. 1a) followed the reaction given by Eq (1). The theoretically available capacity of 1.7 mAh was estimated taking into account polymerization charge of 12 mAh, and theoretical doping degree of 0.33 which stands for one chloride anion per a polymer unit [2, 3, 5, 18, 26]. According to Eq (6), the theoretical mass of the obtained chloride doped PPy for the degree of doping, y = 0.33, was calculated to 14.8 mg with a corresponding specific capacity of as-synthesized polypyrrole of 115 mAh g^{-1}. The theoretical

mass is in an excellent agreement with the experimentally determined of 14.4 mg, giving the current efficiency of the polymerization processes of 97%.

From the cyclic voltammogram, shown in Fig. 1a, can be seen that charge (doping) reaction started at the potential of –0.5 V and proceeded up to ~0.45 V. Above potential of ~0.45 V, overoxidation and possible degradation processes might occur [27, 28]. Discharge (dedoping) process proceeded through a broad potential range of 0.45 to ~ –0.75 V.

Figure 1b shows the optical micrographs of the as synthetized polypyrrole. The morphology of PPy was an open porous 3D structure composed of irregular granular shapes.

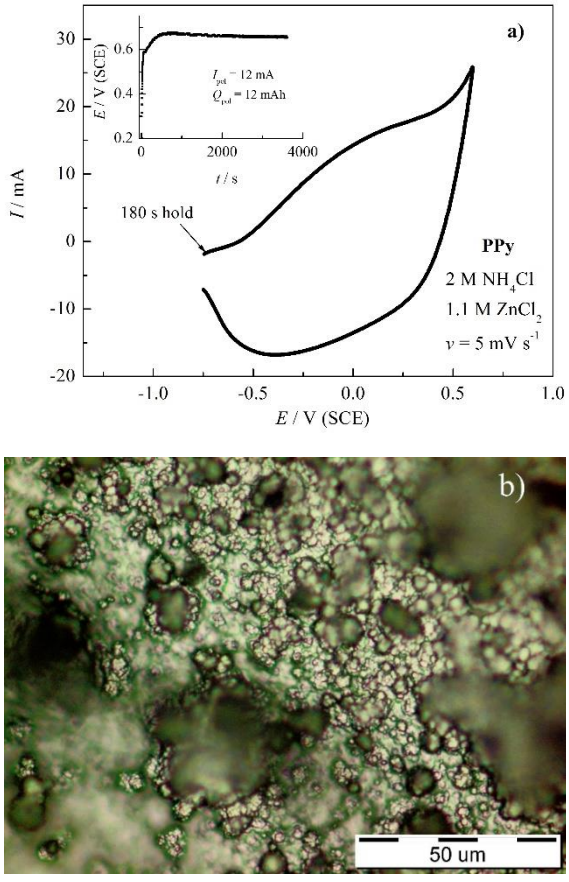

Fig. 1. a) Cyclic voltammogram of the PPy electrode in 2 M NH_4Cl and 1.1 M $ZnCl_2$. Inset: Galvanostatic polymerization of pyrrole from 1 M HCl and 0.1 M pyrrole, b) Optical micrograph of as synthetized PPy from 1 M HCl and 0.1 M pyrrole monomer with polymerization charge of 12 mAh.

In Fig. 2 the polarization curve of the zinc electrode in 2 M NH_4Cl and 1.1 M $ZnCl_2$ was shown. The reversible potential of the zinc electrode was near –1 V. The anodic and cathodic Tafel slopes in the low current density region, e.g. <~10 mA cm^{-2}, were ±36 mV dec^{-1} and for the

higher current density region ±118 mV dec^{-1}. By extrapolating the Tafel slopes to the reversible potential exchange current density of 0.4 mA cm^{-2} was determined. Relatively high exchange current density and low Tafel slopes, suggests that zinc electrode behave in a practically reversible way for the current densities of interest. From the inset in Fig. 2, were anodic and cathodic galvanostatic curves were shown, it can be seen that overpotentials for the deposition and dissolution reaction are very small, between 7 and 15 mV, suggesting that zinc electrode will not have significant influence on the charge/discharge cell voltage.

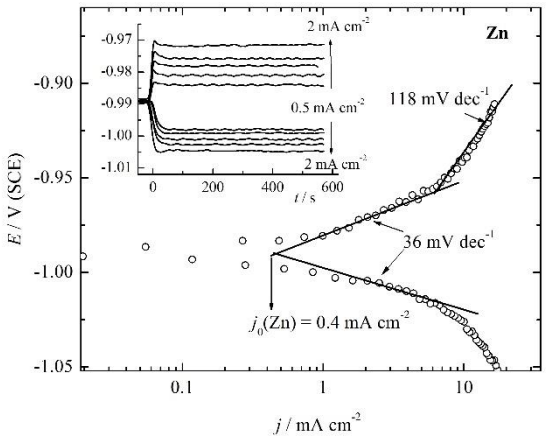

Fig. 2. Polarization curve (v = 1 mV s^{-1}) of the zinc electrode in 2 M NH_4Cl and 1.1 M $ZnCl_2$. Inset: Anodic and cathodic galvanostatic curves for zinc dissolution and deposition for the current densities of: 0.5; 0.75; 1.0; 1.5 and 2.0 mA cm^{-2}.

Figure 3a shows the dependence of the PPy potential during galvanostatic charge-discharge for different applied currents. The charge of the PPy electrode in 2 M NH_4Cl and 1.1 M $ZnCl_2$ occurred continuously in the potential range of ~ –0.4 up to 0.5 V, while discharge takes place practically linearly from 0.35 V to –0.8 V. Simultaneously with the potential of the PPy electrode, the voltage of the Zn-PPy cell was recorded, and the results were shown in Fig 3b. Depending on the applied current, the charge of the cell occurred from ~0.5-0.7 V to 1.5 V. After charge, the open circuit voltage was ~1.3 V. Discharge of the cell starts at 1.3 V and proceed linearly to 0.25 V, followed by a sharp voltage decrease caused by the solid-state diffusion of the chloride anions through PPy film.

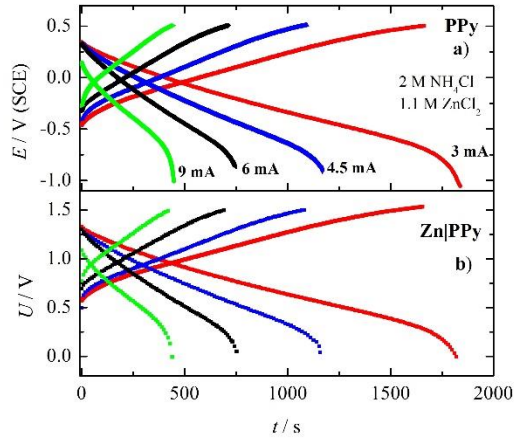

Fig. 3. a) The dependence of the PPy potentials over time on applied currents, b) The dependence of the voltage over time on applied currents of Zn|PPy cell.

The PPy electrode capacity of the charge-discharge for different applied currents was shown in Fig. 4. With increased *Q* rate, from 1.8*Q* to 5.3*Q*, based on the estimated theoretical capacity of 1.7 mAh, the discharge capacity decreases from 1.5 mAh to 1.1 mAh. For the low current, the Coulombic efficiency, C.E., was 108%, and decrease to 100% for the higher discharge rate. Knowing the mass of the PPy of 14.4 mg, the specific capacity was estimated between 105 to 75 mAh g^{-1} of PPy, and the specific currents in the range between 200 to 600 mA g^{-1} of PPy, inset in Fig. 4.

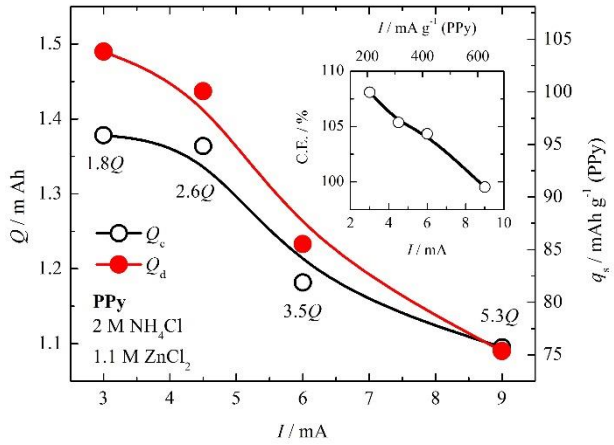

Fig. 4. The dependence of the charge-discharge capacity (left) and specific capacity (right) on applied current. Inset: Coulombic efficiency on applied current and specific current based on PPy mass.

The cyclic behavior was investigated by applying a current of 6 mA over twenty-five cycles, shown in Fig. 5, limiting the PPy charge potential to 0.5 V. It can be seen that slight

changes occurred during cyclization. The charge capacity decreased by 3%, as seen in the Inset of Fig. 5. The observed small increase in the discharge capacity was possibly connected to the expansion of the PPy layer inducing additional sites available for further insertation of the cations at the negative potentials, or to the reduction of the overoxidized polypyrrole backbones.

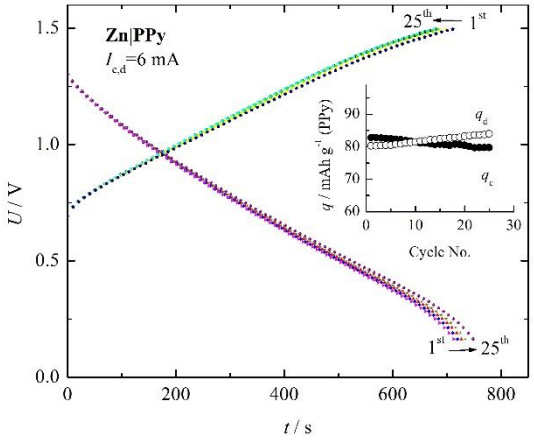

Fig. 5. Cyclization of the Zn|PPy cell. Inset: The dependence of the PPy specific charge-discharge capacity on cycle number.

3.3. Polypyrrole lead systems

Figure 6 shows the synthesis of PPy, PbO_2, and $PbSO_4$ in 1 M H_2SO_4. Electrochemical synthesis of PPy occurred in the potential range of 0.55 to 0.6 V. Based on the Eq. (6) and theoretical doping degree of 0.33, the mass of PPy was calculated to be 4.85 mg, with a corresponding theoretical capacity of 0.76 mAh. Experimentally determined PPy mass was 5.2 mg, giving the current efficiency of the polymerization processes of 107%, which is probably caused by the higher doping degree. The theoretical specific capacity for the sulfate contained solution was valued to 157 mAh g^{-1} of PPy. The lead oxide and lead sulfate were formed through the galvanostatic pattern, as shown in Fig. 6 [21]. Prior to the formation, the electrode was cathodically treated during 300 s to remove naturally formed oxides. Upon application of the anodic current, oxidation of the pure lead to lead sulfate at the potential of -0.55 V, and then the sharp increase of the potential to ~1.85 V, followed by the potential plateau at ~1.55 V can be connected to the transformation of $PbSO_4$ to PbO_2 [21]. The electrode was completely discharged, with the same current, to the potential of -0.6 V. Three cycles of the discharge and charge in 1.0 M H_2SO_4 was used for the formation of lead sulfate, while lead oxide was formed in five cycles of the oxidation/reduction between the potentials of ~ 1 to 1.6 V. Because during the formation of PbO_2, Pb was first converted to $PbSO_4$ that is converted to PbO_2 with the

possibility of oxygen evolution, the active masses were calculated from discharge of the $PbSO_4$ using the Faraday law. For the discharge time of 570 s the mass of $PbSO_4$ is estimated to 5.4 mg which corresponded to 4.3 mg of PbO_2.

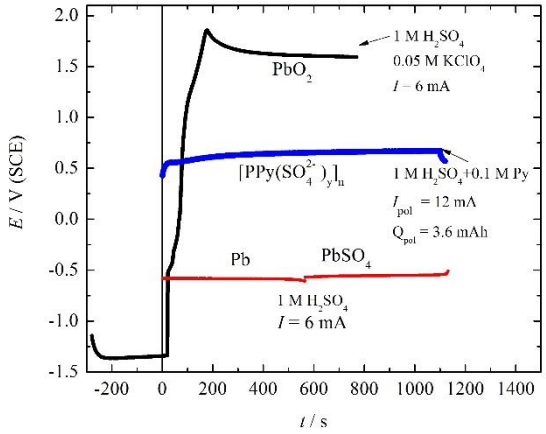

Fig. 6. Electrochemical formation of PPy, PbO_2 and $PbSO_4$

The XRD of the as synthetized PbO_2 corresponds to practically pure β-PbO_2 (JCPDS 41-1492, Plattnerite pdf), which agreed with the data reported by Petersson and Ahlberg [29] who prepared PbO_2 electrode using the similar procedures. The optical micrographs shown in the inset of Fig. 7a, reveals crystalline structure with an average crystal size of ~10 μm. The XDR spectra of as-synthesized lead-lead sulfate was shown in Fig. 7b. The peaks positioned at 2θ of: 31.21°; 36.16°; 52.11° and 62.09° correspond to the pure lead (JCPDS No. 04-0686 Pb pdf), which could be from the bulk of the electrode or more probably from the active mass consisted of Pb+$PbSO_4$. The rest of the observed peaks were in excellent agreement with the peak positions of lead sulfate with anglesite structure (JCPDS No. 36-1461 Anglesite pdf). In the optical micrograph shown in the inset of Fig. 7b, the mixture of the metallic lead crystals with average size of 5 to 10 μm and lead sulfate crystals with similar dimensions can be seen. Figure 7c represents the optical micrograph of as synthetized PPy from 1 M H_2SO_4 and 0.1 M pyrrole monomer with polymerization charge of 3.6 mAh. The morphology of the PPy deposits reminds on the boulder like formations, with some indications of micro-fibrous structures.

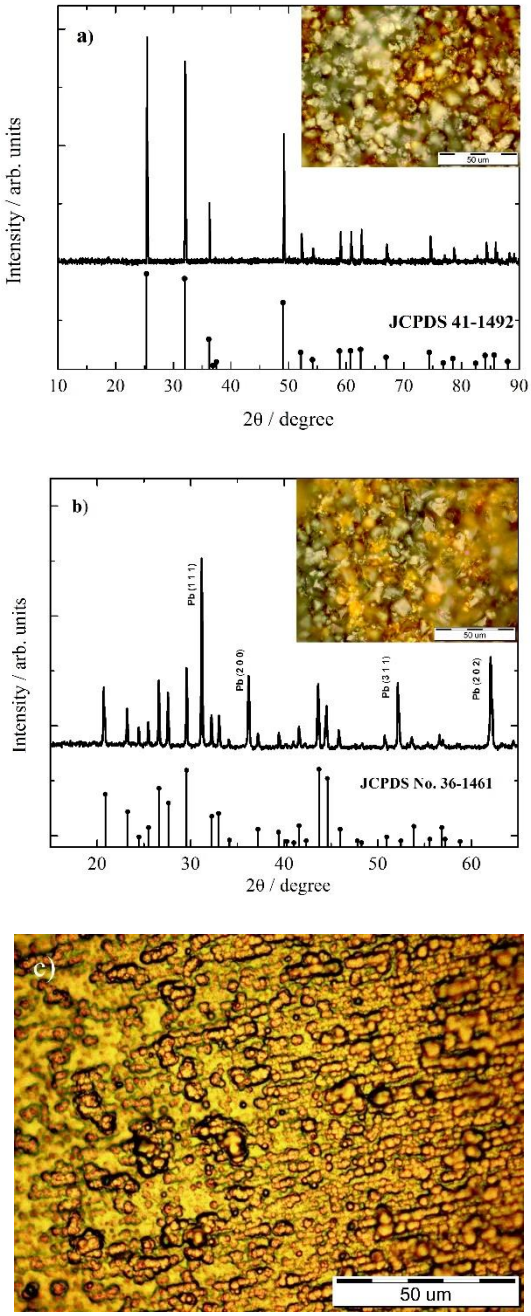

Fig. 7. a) XRD pattern of as synthetized PbO_2. Inset: Optical micrograph of as-synthetized PbO_2. b) XRD pattern of as synthetized $Pb/PbSO_4$. Inset: Optical micrograph of as-synthetized $Pb/PbSO_4$. c) Optical micrograph of as synthetized PPy from 1 M H_2SO_4 and 0.1 M pyrrole monomer with polymerization charge of 3.6 mAh.

The results of the cyclic voltammetry experiments were shown in Fig. 8. As can be seen, PPy electrode possess pseudocapacitive behavior in the broad range of the applied potentials, connected to doping/dedoping processes. Doping by sulfate anions started at -0.4 V and occurred up to the potential of ~0.5 V, followed by the increase of the current density resulted

from the overoxidation process [27, 28]. Dedoping of the PPy electrode occurred in the range of potentials between 0.45 and –0.45 V characterized by a well-defined peak positioned at –0.3 V. Smaller peak in the cathodic part of the voltammogram positioned at potentials more negative than –0.45 V can be assigned to either proton or ammonium cation insertion [30]. Reversible behavior with defined and sharp current peaks, typical to battery electrodes, was observed for the lead-lead sulfate and lead-lead oxide electrodes. Estimated formal potentials for lead-lead sulfate, was -0.58 V and 1.3 V for lead-lead oxide system.

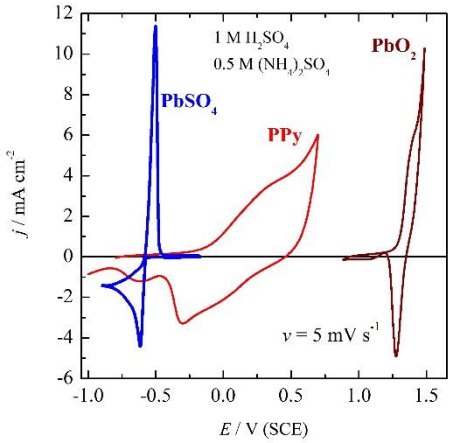

Fig. 8. Cyclic voltammograms of the investigated materials in 1 M H_2SO_4 and 0.5 M $(NH_4)_2SO_4$

Charge/discharge curves obtained with different currents for all investigated electrode materials are given in Fig. 9. Charge, *i.e.* doping of PPy electrode occurred in a wide potential range, starting from –0.1 V and up to 0.55 V, while discharge *i.e.* dedoping occurred in the range between 0.5 V and ~–0.4 V. Faster decrease in the potential, observed below –0.45 V can be connected to the diffusion limitations of anions dedoping and cations insertion in the PPy matrix. Below potentials of ~–1 V the hydrogen evolution reaction occurred. Lead oxide electrode charge was observed in the potential range between 1.4 V and 1.55 V, while discharging was characterized by one flat potential plateau at ~1.3 V. On the other hand, both charge and discharge of the lead sulfate electrode occurred in a narrow potential range between –0.57±0.03 V. As observed, charge and discharge of lead oxide and lead sulfate were slightly dependent on the applied current with determined Coulombic efficiency, C.E., of ~70% for the lead oxide electrode, and ~100% for the lead sulfate respectively. The small Coulombic efficiency of the lead oxide was connected with the charging process [31]. When the lead sulfate is charged to lead oxide at constant current, the charge process can be devided into the three separate regions: efficient C.E. = 100%; mixed C.E. = 50-100% and inefficient C.E. < 50%.

Generally, the “efficient” region is where the of the electrode state of charge, SOC, is below 70-75% and the potential is around 1.4 V. The following, second region of the recharge was “mixed” at the potentials between ~1.4 V and 1.52 V, becouse simultaneously with lead sulfate conversion to lead oxide, oxygen evolution occured decresing the current efficiency. As this stage progressed, a greater and greater portion of the current flowing through the electrode generating oxygen rather than causing useful active material conversion. When the SOC had reached about 90% to 96% at the potentials higher than 1.52 V, the efficiency becomes progressively poorer, and at at 100% SOC the recharge efficiency become zero. Therefore, the overal current efficiency for formation of PbO_2 during charge proces was ~70%. For the transformation of lead sulfate to lead and vice versa during negative electrode charge-discharge no parasitic reactions were present and current efficiency is near 100%.

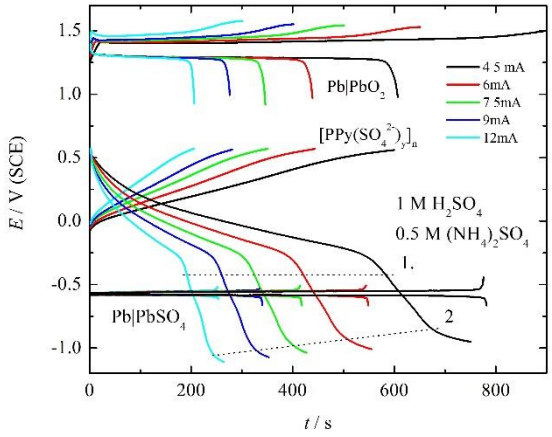

Fig. 9. Charge-discharge curves of the investigated materials for the different currents.

In Fig. 10 the obtained charge-discharge capacity and specific capacity based on PPy mass of 5.2 mg for different applied currents were shown. With increased current, charge capacity slightly decreased from 0.75 mAh (140 mAh g^{-1}) to 0.69 mAh (130 mAh g^{-1}). Discharge capacity for the potential of –0.45 V decreased from 0.73 mAh (134 mAh g^{-1}) to 0.65 mAh (125 mAh g^{-1}), while for the discharge potential of –1 V higher values of capacities, 0.85 mAh (163 mAh g^{-1}) to 0.8 mAh (154 mAh g^{-1}) were obtained. From the inset in Fig. 10, it can be seen that the Coulombic efficiency (C.E.) of the polypyrrole electrode depends on the discharge potentials, and slightly on applied specific current that is in the range of 850 to 2300 mA g^{-1} of PPy. For discharge potentials of –0.45 V, C.E. was around 95%, while for the discharge potentials of ~ –1 V was increased to ~110%, caused most probably due to the possibility of proton or ammonium cation insertion into PPy layer at low potentials [30].

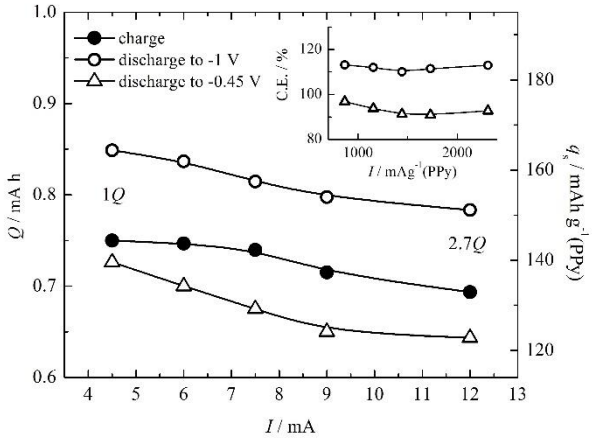

Fig. 10. The dependence of charge-discharge capacity (left) and specific capacity based on PPy mass (right) on applied current. Inset: The dependence of the Coulombic efficiency (C.E.), for PPy end discharge potentials of –1 V (○) and –0.45 V (△), on a specific discharge current.

Figure 11 shows cyclization of the PPy|PbO_2 cell with an applied current of 6 mA. The charge of the cell occurred over a broad voltage range from 0.75 to 2.5 V. Initial increase of the potential from 0.75 V to 1.25 V could be connected with the lead electrode, by the initial conversion of $PbSO_4$ to PbO_2, followed by a plateau in the potential range of 1.25 V to 1.75 V connected with the dedoping of the PPy electrode (see Fig. 9). Next increase of the potential from 1.75 V to 2.35 V was associated with diffusion-controlled anions dedoping from the PPy. Finally, the plateau at ~2.5 V corresponds to hydrogen evolution reaction on the PPy, and $PbSO_4$ remains conversion to PbO_2 associated with the oxygen evolution. After the charge, open circuit voltage was ~1.5 V. Discharge of the cell occurred practically linearly in the voltage range from 1.2 V to ~0.5 V, and during the three cycles, some small decrease of the discharge times in that voltage region was observed. The higher decrease of the discharge time below ~0.5 V can be associated with some small mass differences of PbO_2 electrode during cyclization. Namely, during charge, PPy was dedoped and $PbSO_4$ was converted to PbO_2 with efficiency of approximately 70%. The conversion of $PbSO_4$ to PbO_2 is very complex solid-state diffusion controlled reaction associated with oxygen evolution, which efficiency could vary depending on the prehistory of the electrode [31]. If not all the $PbSO_4$ was converted to PbO_2, due to smaller active PbO_2 mass of the positive electrode, shorter discharge time could provoke fast decrease of the potential. After the prolonged charge (curve 4), the discharge capacity of the cell was recovered. Inset in Fig. 11 shows the dependence of the charge-discharge voltage on specific capacity based on PPy. The full charge process requires ~210 mAh g^{-1} of PPy, while

obtained discharge capacity of 152 mAh g^{-1} of PPy was in excellent agreement with theoretically predicted one of 157 mAh g^{-1}.

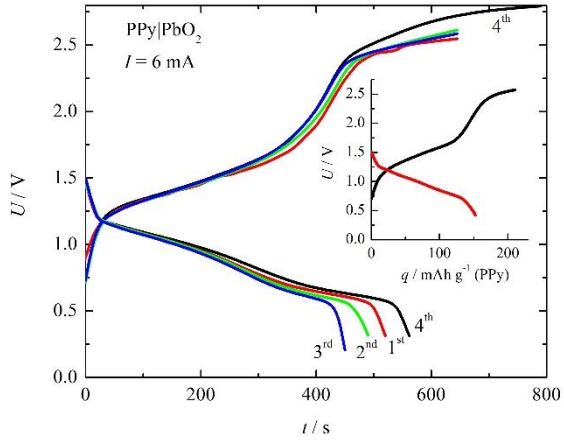

Fig. 11. Cyclization of the PPy|PbO_2 cell with an applied current of 6 mA. Inset: dependence of the charge-discharge voltage on specific capacity based on PPy.

Figure 12 shows the cyclization of the Pb|PPy cell over 20 cycles. During cyclization, practically no significant changes of the charge-discharge curves were observed. Charge occurred linearly in the voltage range between ~0.6 V to 1.1 V, while discharge proceeds from 1.05 V to ~0.4 V, followed by a fast drop of the voltage due to diffusion limitation. Inset in Fig. 10 represents the dependence of the charge-discharge voltage on specific capacity based on PPy. Charge capacity was in the range of 142 mAh g^{-1} of PPy, while useful discharge capacity was ~120 mAh g^{-1} of PPy.

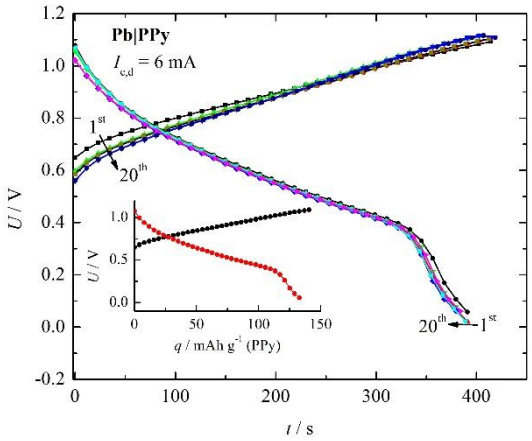

Fig. 12. Cyclization of the $PbSO_4$|PPy cell with an applied current of 6 mA. Inset: dependence of the charge-discharge voltage on specific capacity based on PPy

3.4. Electrochemical and electrical characteristics of the cells

For the considered systems, the half-cell and overall discharge reactions were given by the following equations:

Zinc-polypyrrole:

$[PPy^{y+}(Cl^-)_y]_n + yne = [PPy]_n + nyCl^-$

$Zn = Zn^{2+} + 2e$

$2[PPy^{y+}(Cl^-)_y]_n + nyZn = 2[PPy]_n + 2nyCl^- + nyZn^{2+}$

Polypyrrole-lead oxide:

$PbO_2 + 4H^+ + SO_4^{2-} + 2e = PbSO_4 + 2H_2O$

$[PPy]_n + nySO_4^{2-} = [PPy^{2y+}(SO_4^{2-})_y]_n + 2yne$

$[PPy]_n + 2nyH_2SO_4 + ynPbO_2 = [PPy^{2y+}(SO_4^{2-})_y]_n + nyPbSO_4 + 2nyH_2O$

Lead sulfate-polypyrrole:

$[PPy^{2y+}(SO_4^{2-})_y]_n + 2yne = [PPy]_n + nySO_4^{2-}$

$Pb + SO_4^{2-} = PbSO_4 + 2e$

$[PPy^{2y+}(SO_4^{2-})_y]_n + nyPb = [PPy]_n + nyPbSO_4$

From the discharge reactions, it can be seen that for the Zn|PPy system, concentrations of the chloride ions in solution increased, for PPy|PbO_2 like as in classical lead-acid battery concentration of the sulfuric acid decreased [32], while the $PbSO_4$|PPy behave as a "rocking chair" battery [33] without sulfate concentrations change during discharge-charge processes.
To determine the possible electrical characteristic, the dependence of the charge-discharge voltages on specific capacities for the current of 6 mA (1 mA cm^{-2}), of investigated cells were compared and shown in Fig. 13. Specific capacities were recalculated from Figs. 5, 11 and 12 (multiplying current with charge and discharge times) according to the equation:

$$q_d = \frac{I_{c,d} \times t_{c,d}}{m_{am}} \quad (8)$$

where m_{am} was the active masses of the electrodes involved in the reactions, given as:

$$m_{am} = m(\mathrm{PPy}) + m(\mathrm{X}) \tag{9}$$

m(X) was the mass of Zn, $PbSO_4$ or PbO_2 during charge or discharge processes, respectively, calculated independently for discharge and charge using the Faraday law:

$$m(\mathrm{X})_{c,d} = \frac{I_{c,d} t_{c,d} M(\mathrm{X})}{nF} \tag{10}$$

where M(X) is the molar mass of Zn = 65.38 g mol^{-1}; PbO_2 = 239.2 g mol^{-1} and $PbSO_4$ = 303.26 g mol^{-1}. Specific values were calculated using the active masses of: m[PPy(Cl^-)] = 14.4 mg, m[PPy(SO_4^{2-})] = 5.2 mg, m(PbO_2) = 3.9 mg and m($PbSO_4$) = 3.7 mg. which participated in the reactions.

The specific discharge capacitance was calculated from the slopes, (dU/dt), of the linear part of the discharge curves:

$$C_d = \frac{I_d}{(\mathrm{d}U / \mathrm{d}t) m_{am}} \tag{11}$$

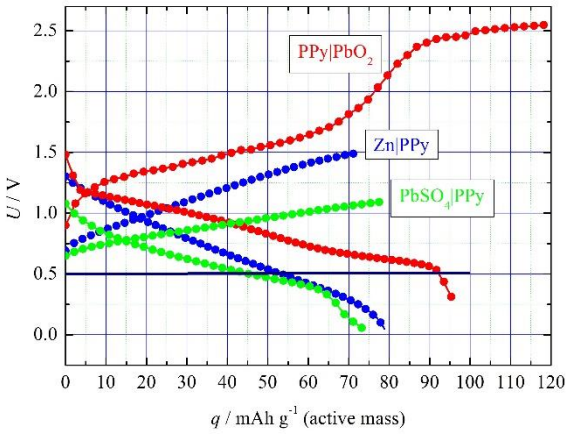

Fig. 13. The dependence of the charge-discharge voltages on the specific capacities based on active masses at a current of 6 mA (1 mA cm^{-2}), of the investigated cells.

Useful specific discharge energy was obtained by integrating the dependence of the voltage over the specific capacity from open circuit voltage to the voltage of 0.5 V, which could be considered as a minimum voltage to any practical application, according to:

$$w_d = \int_{U=0.5}^{U_0} U_d \mathrm{d}q \tag{12}$$

while specific charge energy was calculated by integration of the complete charge curve. Energy efficiency, which is one of the most important parameters considering the required energy for charge and obtained useful energy during discharge, was calculated according to:

$$\eta_w = \frac{w_c}{w_d} \times 100 \quad (13)$$

The calculated electrical parameters were summarized in Table 1. From Table 1 it can be seen that the open circuit voltage, average discharge voltage, and the specific discharge capacity of the cells were as follows: 1.3 V, 0.85 V and 54 mAh g^{-1} for Zn|PPy cell; 1.5 V, 0.9 V and 92 mAh g^{-1} for PPy|PbO_2 cell, while for the $PbSO_4$|PPy cell 1.1 V, 0.65 V and 47 mAh g^{-1}. Specific discharge energy to the beneficial discharge potentials of ~0.5 V, and charge-discharge energy efficiency was estimated to 46 mWh g^{-1} (55%), 80 mWh g^{-1} (38%), and 34 mWh g^{-1} (59%) for the considered systems, respectively.

Table 1. Electrical characteristics of the investigated cells for current of 6 mA: Open circuit voltage, U_0; average discharge voltage, U_{av}; specific discharge current, I_d; specific discharge capacitance, C_d; specific discharge capacity, q_d; specific discharge energy, w_d to 0.5 V; specific charge energy, w_c; energy efficiency, η_w, and specific discharge power, P_d to 0.5 V.

System	U_0 V	U_{av} V	I_d A g^{-1}	C_d F g^{-1}	q_d mAh g^{-1}	w_d mWh g^{-1}	w_c mWh g^{-1}	η_w %	P_d mW g^{-1}
Zn|PPy	1.3	0.85	0.38	265	54	46	83	55	329
PPy|PbO_2	1.5	0.9	0.66	504	92	80	214	38	571
$PbSO_4$|PPy	1.1	0.65	0.67	414	47	34	70	49	490

Obtained specific capacity and energy was in the range of classical battery systems, but much higher than that reported for supercapacitors, which are in the range of 1 to 10 mWh g^{-1} [34, 35]. The specific capacitance was 265 F g^{-1} for Zn|PPy, 504 F g^{-1} for PPy|PbO_2 and 414 F g^{-1} for $PbSO_4$|PPy systems. Because battery systems suffer from low power contents, typically 20 to 100 mW g^{-1} [36], the specific power of the investigated cell was also estimated. In that manner, the specific discharge energy was converted from mWh g^{-1} to mWs g^{-1} multiplying with 3600 s h^{-1}, and dividing with discharge times to 0.5 V, determined from Figs. 5, 11 and 12. As can be seen from Table 1 power contents of 330-570 mW g^{-1} were much higher than in classical battery systems. Considering the estimated specific power and energy, investigated systems could be classified as “supercapattery” (**supercapa**citors -ba**tteries**) [37, 38].

4. Conclusions

The electrochemical and electrical characteristics of the cells based on polypyrrole in combination with zinc, lead oxide, and lead sulfate were determined. The Zn|PPy cell in 2 M NH_4Cl with 1.1 M $ZnCl_2$ electrolyte had the open circuit voltage of 1.3 V, average discharge voltage of 0.85 V and specific discharge capacity of 54 mAh g^{-1}. The PPy|PbO_2 cell in 1 M H_2SO_4 with 0.5 M $(NH_4)_2SO_4$ electrolyte had the open circuit voltage of 1.5 V, the average discharge voltage of 0.9 V, and specific discharge capacity of 92 mAh g^{-1}. The $PbSO_4$|PPy cell in the same electrolyte had the open circuit voltage of 1.1 V, average discharge voltage of 0.65 V and specific discharge capacity of 47 mAh g^{-1}. The specific discharge energy to the useful discharge potentials of ~0.5 V, charge-discharge energy efficiency, as well as specific power, were estimated to 46 mWh g^{-1} (55%), 329 mW g^{-1} for Zn|PPy cell; 80 mWh g^{-1} (38%), 571 for PPy|PbO_2 cell, and 34 mWh g^{-1} (49%), 490 mW g^{-1} for $PbSO_4$|PPy cell. Based on estimated specific energy and power, it was suggested that investigated cells could be classified as "supercapattery" type of the electrochemical power sources.

Acknowledgment

The work was supported by the Ministry of Education and Science of the Republic of Serbia under the research project ON172046.

Data availability

The processed data required to reproduce these findings are available to download from: https://data.mendeley.com/datasets/n8fcg2g5z4/1

References

[1] R. De Surville, M. Jozefowicz, L.T. Yu, J. Perichon, R. Bwet, Electrochemical chains using protolytic organic semiconductors, Electrochim. Acta 13 (1968) 1451-1458.
[2] P. Novák, K. Müller, K.S.V. Santhanam, O. Haas, Electrochemically active polymers for rechargeable batteries, Chem. Rev. 97 (1997) 207-281.
[3] R. Holze, Y.P. Wu, Intrinsically conducting polymers in electrochemical energy technology: Trends and progress, Electrochim. Acta 122 (2014) 93-107.
[4] G.A. Snook, P. Kao, A.S. Best, Conducting-polymer-based supercapacitor devices and electrodes, J. Power Sources 196 (2011) 1-12.
[5] R. Ramya, R. Sivasubramanian, M.V. Sangaranarayanan, Conducting polymers-based electrochemical supercapacitors-Progress and prospects, Electrochim. Acta 101 (2013) 109-129.

[6] S. Li, Z.P. Guo, C.Y. Wang, G.G. Wallace, H.K. Liu, Flexible cellulose based polypyrrole–multiwalled carbon nanotube films for bio-compatible zinc batteries activated by simulated body fluids, J. Mater. Chem. A. 1 (2013) 14300-14305.
[7] S. Li, K. Shu, C. Zhao, C. Wang, Z. Guo, G. Wallace, H.K. Liu, One-step synthesis of graphene/polypyrrole nanofiber composites as cathode material for a biocompatible zinc/polymer battery, ACS Appl. Mater. Interfaces 6 (2014) 16679-16686.
[8] S. Li, I. Sultana, Z. Guo, C. Wang, G.G. Wallace, H-K. Liu, Polypyrrole as cathode materials for Zn-polymer battery with various biocompatible aqueous electrolytes, Electrochim. Acta 95 (2013) 212-217.
[9] G. Nyström, A. Razaq, M. Strømmev L. Nyholm, A. Mihranyan, Ultrafast all-polymer paper-based batteries, Nano Lett. 9 (10) (2009) 3635-3639.
[10] H. Manjunatha, G.S. Suresh, T.V. Venkatesha, Electrode materials for aqueous rechargeable lithium batteries, J. Solid State Electrochem. 15 (2011) 431–445.
[11] G. Wang, Q. Qu, B. Wang, Y. Shi, S. Tian, Y. Wu, An aqueous electrochemical energy storage system based on doping and intercalation: Ppy/$LiMn_2O_4$, Chem. Phys. Chem. 9 (2008) 2299-2301.
[12] G.J. Wang, L.C. Yang, Q.T. Qu, B. Wang, Y.P. Wu, R. Holze, An aqueous rechargeable lithium battery based on doping and intercalation mechanisms, J. Solid State Electrochem. 14 (2010) 865-869.
[13] W. Tang, L. Liu, Y. Zhu, H. Sun, Y. Wu, K. Zhu, An aqueous rechargeable lithium battery of excellent rate capability based on a nanocomposite of MoO_3 coated with PPy and LiMn2O4, Energy Environ. Sci. 5 (2012) 6909-6913.
[14] W. Tang, X.W. Gao, Y.S. Zhu, Y.B. Yue, Y. Shi, Y.P. Wu, K. Zhu, A hybrid of V_2O_5 nanowires and MWCNTs coated with polypyrrole as an anode material for aqueous rechargeable lithium batteries with excellent cycling performance, J. Mater. Chem. 22 (2012) 20143-20145.
[15] L.L. Liu, X.J. Wang, Y.S. Zhu, C.L. Hu, Y.P. Wu, R. Holze, Polypyrrole-coated LiV_3O_8-nanocomposites with good electrochemical performance as anode material for aqueous rechargeable lithium batteries, J. Power Sources 224 (2013) 290-294.
[16] G. G.Wallace, G. Tsekouras, C. Wang, (2010) Inherently Conducting Polymers via Electropolymerization for Energy Conversion and Storage, in Electropolymerization: Concepts, Materials and Applications (eds S. Cosnier and A. Karyakin), Wiley-VCH Verlag GmbH & Co. KGaA, Weinheim, ch11
[17] B.N. Grgur, M.M. Gvozdenović, J. Stevanovic, B.Z. Jugovic, V.M. Marinovic, Polypyrrole as possible electrode materials for the aqueous-based rechargeable zinc batteries, Electrochim. Acta 53 (2008) 4627-4632.
[18] B.N. Grgur, Metal | polypyrrole battery with the air regenerated positive electrode, J. Power Sources, 272 (2014) 1053-1060.
[19] A.A. Alguail, A.H. Al-Eggiely, M.M. Gvozdenović, B.Z. Jugović, B.N. Grgur, Battery type hybrid supercapacitor based on polypyrrole and lead-lead sulfate, J. Power Sources, 313 (2016) 240-246.
[20] D. P. Dubal, O. Ayyad, V. Ruiz, P. Gómez-Romero, Hybrid energy storage: the merging of battery and supercapacitor chemistries, Chem. Soc. Rev., 44 (2015) 1777-1790.
[21] B.N. Grgur, A. Žeradjanin, M.M. Gvozdenović, M.D. Maksimović, T.Lj. Trišović, B.Z. Jugović, Electrochemical characteristics of rechargeable polyaniline/lead dioxide cell, J. Power Sources 217 (2012) 193-198.
[22] S. Suematsu, Y. Oura, H. Tsujimoto, H. Kanno, K. Naoi, Conducting polymer films of cross-linked structure and their QCM analysis, Electrochim. Acta 45 (2000) 3813–3821.
[23] E M Genies, G Bidan, A F Diaz, Spectroelectrochemical study of polypyrrole films, J. Electroanal. Chem. 149 (1983) 101-113.

[24] T.V. Vernitskaya, O.N. Efimov, Polypyrrole: a conducting polymer; its synthesis, properties, and applications, Russ. Chem. Rev. 66 (5) (1997) 443-457.
[25] W. Su, J.O. Iroh, Formation of polypyrrole coatings on stainless steel in aqueous benzene sulfonate solution, Electrochim. Acta, 42 (17) (1997) 2685-2694.
[26] P.M. Carrasco, M. Cortazar, E. Ochoteco, E. Calahorra, J.A. Pomposo1, Comparison of surface and bulk doping levels in chemical polypyrroles of low, medium and high conductivity, Surf. Interface Anal. 39 (2007) 26-32.
[27] R. Mazeikiene, A. Malinauskas, Kinetics of the electrochemical degradation of polypyrrole, Polym. Degrad. Stab. 75 (2002) 255-258.
[28] Y. Li, R. Qian, Electrochemical overoxidation of conducting polypyrrole nitrate film in aqueous solutions, Electrochim. Acta 45 (2000) 1727-1731.
[29] I. Petersson, E. Ahlberg, On the question of electrochemical activity of differently formed lead dioxides, Journal of Power Sources 91 (2000) 137–142.
[30] C. Weidlich, K.-M. Mangold, K. Jüttner, EQCM study of the ion exchange behaviour of polypyrrole with different counter ions in different electrolytes, Electrochim. Acta 50 (2005) 1547-1552.
[31] R. Kaushik, I. G. Mawston, Coulombic efficiency of lead/acid batteries, particularly in remote-area power-supply (RAPS) systems, J. Power Sources, 35 (1991) 377-383.
[32] D. Linden, T.B. Reddy (Eds.), Handbook of Batteries (third ed.), McGraw-Hill, New York (2001) Ch. 23.
[33] B. Scrosati, Lithium rocking chair batteries: An old concept? J. Electrochem. Soc. 139 (10) (1992) 2776-2781.
[34] A.K. Shukla, A. Banerjee, M.K. Ravikumar, A. Jalajakshi, Electrochemical capacitors: Technical challenges and prognosis for future markets, Electrochim. Acta 84 (2012) 165–173.
[35] D. Cericola, R. Kötz, Hybridization of rechargeable batteries and electrochemical capacitors: Principles and limits, Electrochim. Acta 72 (2012) 1– 17.
[36] X. Zhao, B. Mendoza Sánchez, P.J. Dobson, P.S. Grant, The role of nanomaterials in redox-based supercapacitors for next generation energy storage devices, Nanoscale 3 (2011) 839–855.
[37] L. Yu, G.Z. Chen, Redox electrode materials for supercapatteries, J. Power Source, 326 (2016) 604–612.
[38] L. Yua, G.Z. Chen, High energy supercapattery with an ionic liquid solution of $LiClO_4$, Faraday Discuss., 190 (2016) 231-240.